

Incompressibility and Hardness of Solid Solution Transition Metal Diborides: $\text{Os}_{1-x}\text{Ru}_x\text{B}_2$

Michelle B. Weinberger,^{†,‡} Jonathan B. Levine,[†] Hsiu-Ying Chung,[§]
Robert W. Cumberland,^{†,⊥} Haider I. Rasool,[†] Jenn-Ming Yang,[§] Richard B. Kaner,^{*,†} and
Sarah H. Tolbert^{*,†}

*Department of Chemistry and Biochemistry and Department of Materials Science and Engineering,
University of California, Los Angeles, California 90095*

Received January 23, 2009. Revised Manuscript Received March 12, 2009

Interest in new ultraincompressible hard materials has prompted studies of transition metal diboride solid solutions. We have synthesized pure RuB_2 and solid solutions of $\text{Os}_{1-x}\text{Ru}_x\text{B}_2$. The mechanical properties of these materials are investigated using in situ high-pressure X-ray diffraction and Vickers hardness testing techniques. Both bulk moduli and hardness vary linearly with composition in accordance with Vegard's law, whereas the differing behavior among end-members can be explained by relativistic effects, core electron density, and differences in the cohesive energy of the parent metals. The results provide a refinement of the rules previously reported for the design of new superhard materials.

Introduction

The development of new superhard materials is driven by the need for chemically diverse, robust materials for abrasives, cutting tools, and coatings for industrial applications. In recent years, we have focused on the development of a new class of transition metal diborides that utilize highly incompressible second- and third-row transition metals to satisfy these requirements. In this paper, we explore the effects of atomic scale substitution on the mechanical properties of these compounds.

Diamond has traditionally been considered the best option for fulfilling industrial cutting requirements. Its remarkable hardness and general chemical inertness make it widely applicable. However, there are situations where materials with alternate chemical compositions outperform diamond. For example, diamond cannot be used to cut steel or other ferrous metals because of the formation of iron carbide at elevated temperatures. For this application, materials with different chemical and mechanical properties are desirable.

In designing new materials for such applications, we want to optimize both incompressibility and hardness. Hardness has been the traditional gauge of a material's mechanical strength, and the relationships between hardness, shear strength, incompressibility, and Young's modulus have been studied extensively.^{1–4} Understanding the connections between these properties is an important aspect of predicting

new, potentially superhard materials. Diamond has high shear strength, high Young's modulus, high hardness, and high incompressibility, and it is useful to consider how its chemistry gives rise to these mechanical properties. Diamond's phenomenal incompressibility can be attributed to its high valence electron density (VED), which has been shown to be a principle factor for determining bulk modulus.^{2,5} Due in part to the small size of the carbon atom, diamond has the highest VED of any known material, 0.705 electrons/Å³. When diamond is compressed elastically and hydrostatically, the energetically unfavorable electronic repulsions result in the highest measured bulk modulus, 442 GPa.⁶ Hardness, i.e., resistance to plastic deformation, on the other hand, requires short, covalent bonds.⁴ The structure of diamond, with its three-dimensional network of covalent bonds, successfully inhibits the formation and propagation of dislocations, resulting in diamond's exceptional hardness (~100 GPa).⁷ Therefore, in our quest to design ultraincompressible, hard materials, we have applied two design parameters: high valence electron density and the incorporation of bond covalency.⁸

Recently, osmium has been extensively studied with several publications reporting an exceptionally high experimentally determined bulk modulus.^{9–12} Moreover, our own strength studies of osmium revealed that osmium is the

* To whom correspondence should be addressed. E-mail: tolbert@chem.ucla.edu (S.H.T.); kaner@chem.ucla.edu (R.B.K.).

[†] Department of Chemistry and Biochemistry, University of California, Los Angeles.

[‡] Current address: Geophysical Laboratory at the Carnegie Institution of Washington Washington, D.C., 20015.

[§] Department of Materials Science and Engineering, University of California, Los Angeles.

[⊥] Current address: HRL Laboratories LLC, Malibu, CA 90265.

(1) Chung, H.-Y.; Weinberger, M. B.; Yang, J.-M.; Tolbert, S. H.; Kaner, R. B. *Appl. Phys. Lett.* **2008**, *92*, 261904.

(2) Gilman, J. J., *Electronic Basis of the Strength of Materials*; Cambridge University Press: Cambridge, U.K., 2003.

(3) Kaner, R. B.; Gilman, J. J.; Tolbert, S. H. *Science* **2005**, *308* (5726), 1268–1269.

(4) Teter, D. M. *MRS Bull.* **1998**, *23*, 22.

(5) Gilman, J. J.; Cumberland, R. W.; Kaner, R. B. *Int. J. Refract. Met. Hard Mater.* **2006**, *24*, 1–5.

(6) Aleksandrov, I. V.; Goncharov, A. F.; Zisman, A. N.; Stishov, S. M. *Zh. Eksp. I Teor. Fiz.* **1987**, *93* (2), 680–691.

(7) Cohen, M. L. *Science* **1993**, *261*, 307.

(8) Cumberland, R. W.; Weinberger, M. B.; Gilman, J. J.; Clark, S. M.; Tolbert, S. H.; Kaner, R. B. *J. Am. Chem. Soc.* **2005**, *127* (20), 7264–7265.

(9) Cynn, H.; Klepeis, J. E.; Yoo, C.-S.; Young, D. A. *Phys. Rev. Lett.* **2002**, *88* (13), 135701/1–135701/4.

(10) Kenichi, T. *Phys. Rev. B* **2004**, *70* (1), 012101/1–012101/4.

strongest metal ever studied under non-hydrostatic stress, further supporting its use as a host matrix for this new class of ultra-incompressible borides.¹³ Like diamond, osmium metal has a high valence electron density, 0.572 electrons/Å³, resulting in a bulk modulus between 395 and 462 GPa.^{9–11} Although its hexagonal close-packed (hcp) crystal structure resists elastic compression, the metallic bonding offers little resistance to the motion of dislocations.² Consequently, although the bulk modulus is high, the hardness of osmium is very low, only 3.9 GPa.¹⁴

This hardness can be improved with the addition of a light main group element to the structure. In the synthesis of osmium diboride, boron is incorporated into the interstitial sites, which comprise 26 volume percent of osmium's crystal lattice.¹⁵ Formation of osmium diboride is accompanied by a distortion of the hcp host matrix crystal structure to an orthorhombic one. Through this process, covalent bonding is introduced between the metal and boron atoms, whereas the valence electron density remains essentially unchanged.^{16,17} The presence of covalent bonds increases the hardness from 3.9 GPa for pure osmium to 37 GPa for OsB₂, without substantially reducing the bulk modulus (365–395 GPa).^{8,18} However, although 37 GPa is high, it does not constitute a “superhard” material.¹⁹ This categorization requires a hardness of 40 GPa or higher. One reason for the lower hardness of OsB₂ compared to superhard ReB₂,²⁰ for example, could be the presence of a double layer of metal atoms between each boron layer in the crystal structure that reduces the resistance to shear deformation.¹⁹ Thus we sought to use atomic scale substitution to both learn about atom specific effects on hardness and to further improve the hardness of this material.

To understand solid solution hardening it is necessary to first understand the mechanics of plastic deformation. When stress is applied to a crystal beyond its elastic limit (e.g., during hardness indentation testing), the material distorts by plastic deformation through the formation and movement of dislocations.²¹ These dislocations, however, do not move concertedly through a lattice. Instead, small sections, called kinks, move stepwise in a direction parallel to the normal vector simply by breaking one bond and forming another.²² Dislocation mobility in covalently bonded crystals, such as

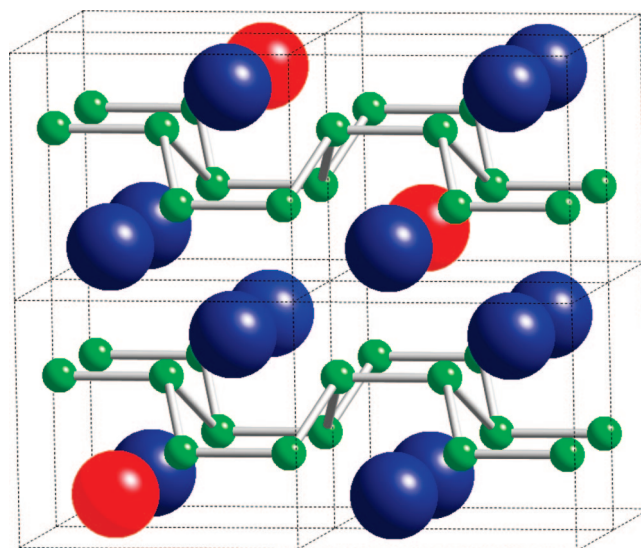


Figure 1. Eight stacked unit cells of Os_xRu_{1-x}B₂. The large blue spheres represent osmium atoms, whereas the small green spheres represent boron atoms. The red spheres correspond to ruthenium atoms that have been incorporated into the structure by randomly replacing osmium atoms.

OsB₂, is therefore determined by the bonding interactions between the kinks and near neighbor atoms. The stress necessary to move a kink from one atom to the next (and subsequently further along in the lattice) depends on the local energy gradient present.^{22,23}

Generally, dislocation kinks are fairly mobile because the electrostatic forces are equivalent on either side of the kink. These symmetric forces allow for easy translation of the kink bond from one atom to the next, i.e., moving a bond from one osmium atom to the next osmium atom in OsB₂. This homogeneity can be disrupted with the substitution of one element in the lattice for another to create a solid solution. By changing the energy profile of neighboring atoms, kink motion becomes an asymmetric process, thus impeding dislocation mobility. To compensate for this modified energy barrier, higher stress levels are required to induce deformation. Thus, the hardness of the material increases. La_{1-x}Ce_xB₆, Nb_{1-x}Zr_xC and TiC_xN_{1-x} are just a few examples of solid-solution hardening that have been reported in the literature.^{23,24}

To test this theory and potentially improve the hardness of OsB₂, we have synthesized solid solutions of Os_{1-x}Ru_xB₂ by randomly substituting ruthenium metal for osmium in OsB₂ (Figure 1). Ruthenium was chosen because of its close proximity to osmium in the periodic table, its similar size, and the fact that RuB₂ also adopts an orthorhombic crystal structure. All of these characteristics suggest a potential for elemental mixing over a broad range of concentrations. A total of three solid solutions were synthesized corresponding to the following nominal compositions, Os_{1-x}Ru_xB₂, $x = 0.2, 0.5, \text{ and } 0.7$, and studied by high pressure X-ray diffraction and microindentation. To understand the behavior of the solid solutions, it is necessary to characterize the behavior of the pure end members. OsB₂ has been extensively investigated;

(11) Occelli, F.; Farber Daniel, L.; Badro, J.; Aracne Chantel, M.; Teter David, M.; Hanfland, M.; Canny, B.; Couzinet, B. *Phys. Rev. Lett.* **2004**, *93* (9), 095502.

(12) Voronin, G. A.; Pantea, C.; Zerda, T. W.; Wang, L.; Zhao, Y. *J. Phys. Chem. Solids* **2005**, *66* (5), 706–710.

(13) Weinberger, M. B.; Tolbert, S. H.; Kavner, A. *Phys. Rev. Lett.* **2008**, *100*, 045506.

(14) Shackelford, J. F.; Alexander, W., *CRC Handbook of Materials Science & Engineering* 3rd ed.; CRC Press: Boca Raton, FL, 2001.

(15) Aronsson, B. *Acta Chem. Scand.* **1963**, *17* (7), 2036–50.

(16) Chen, Z. Y.; Xiang, H. J.; Yang, J.; Hou, J. G.; Zhu, Q. *Phys. Rev. B* **2006**, *74* (1), 012102/1–012102/4.

(17) Chiodo, S.; Gotsis, H. J.; Russo, N.; Sicilia, E. *Chem. Phys. Lett.* **2006**, *425* (4–6), 311–314.

(18) Chung, H.-Y.; Yang, J. M.; Tolbert, S. H.; Kaner, R. B. *J. Mater. Res.* **2008**, *23* (6), 1797–1801.

(19) Yang, J.; Sun, H.; Chen, C. *J. Am. Chem. Soc.* **2008**, *130* (23), 7200–7201.

(20) Chung, H.-Y.; Weinberger, M. B.; Levine, J. B.; Kavner, A.; Yang, J.-M.; Tolbert, S. H.; Kaner, R. B. *Science* **2007**, *316* (5823), 436–439.

(21) Ashby, M. F. *Philos. Mag.* **1970**, *21* (170), 399.

(22) Gilman, J. J. *Mater. Sci. Eng., A* **1996**, *209* (1–2), 74–81.

(23) Jhi, S. H.; Ihm, J.; Louie, S. G.; Cohen, M. L. *Nature (London)* **1999**, *399* (6732), 132–134.

(24) Korsukova, M. M.; Gurin, V. N.; Otani, S.; Ishizawa, Y. *Solid State Commun.* **1996**, *99* (4), 215–219.

however, the properties of RuB_2 have not yet been sufficiently characterized.^{1,8,18,25} Therefore, we have also studied RuB_2 via in situ high-pressure X-ray diffraction and micro-indentation experiments.

Experimental Section

Two methods were employed in the synthesis of RuB_2 . In the first method, ruthenium was mixed with 4 moles of boron and heated at 1000 °C for 5 days under a vacuum, producing phase-pure crystalline RuB_2 with 2 moles of amorphous boron remaining as an impurity. In the second method, ruthenium and boron powders were mixed together, pressed into a pellet, and then liquefied using a 3 phase arc melter with a water-cooled copper hearth under an argon atmosphere in accordance with the synthesis reported by Aronsson.¹⁵ The result was a solid, metallic ingot of RuB_2 that could be used for hardness testing. All of the solid solutions were synthesized via arc-melting. Ambient pressure powder X-ray diffraction patterns were collected on a XPert Pro powder diffractometer (PANalytical) with $Cu\ K\alpha$ radiation ($\lambda = 1.5418\ \text{\AA}$). Elemental analysis was performed using a JSM-6700F field-emission scanning electron microscope (JEOL Ltd.) equipped with an energy-dispersive X-ray spectroscopy detector (EDAX) utilizing a super ultrathin detector window.

In situ high pressure X-ray diffraction experiments were performed at the Advanced Light Source at Lawrence Berkeley National Laboratory on beamline 11.3.1. RuB_2 , $Os_{0.8}Ru_{0.2}B_2$ and $Os_{0.5}Ru_{0.5}B_2$ powders were individually compressed quasi-hydrostatically in a Diacell gas membrane pressurized diamond anvil cell up to 28 GPa. Ethylcyclohexane was used as the pressure-distributing medium. Diffraction patterns were collected in situ at elevated pressures and were analyzed via a Rietveld refinement procedure using GSAS.²⁶ To eliminate the necessity of removing the diamond anvil cell from the beamline to determine the pressure of each data set, we homogeneously distributed sodium chloride throughout the sample in the cell. Because the equation of state of sodium chloride has been studied extensively, it can be used as a pressure calibrant.²⁷

Microindentation experiments were performed using a Vickers diamond microindenter (Buehler, Ltd.). The samples were encased in a slow-curing epoxy resin and preliminary polishing was carried out using silicon carbide abrasive paper. Diamond films (30, 15, 6, 3, and 1 μm particle sizes) were used for fine polishing in order to obtain a mirror finish. A minimum of 10 indentations were made on each sample at varying loads between 0.25 and 1.96 N. The residual indentation diagonal lengths were measured using an Axiotech 100 reflected-light microscope (Carl Zeiss, Inc.) under 500 \times magnification. Vickers microhardness (H_v) was calculated using eq 1:

$$H_v = 1854.4P/d^2 \quad (1)$$

where d is the arithmetic mean of the two diagonals of the indentation and P is the applied load.

Results and Discussion

The powder diffraction patterns of RuB_2 synthesized via arc-melting and from the furnace reaction revealed that the

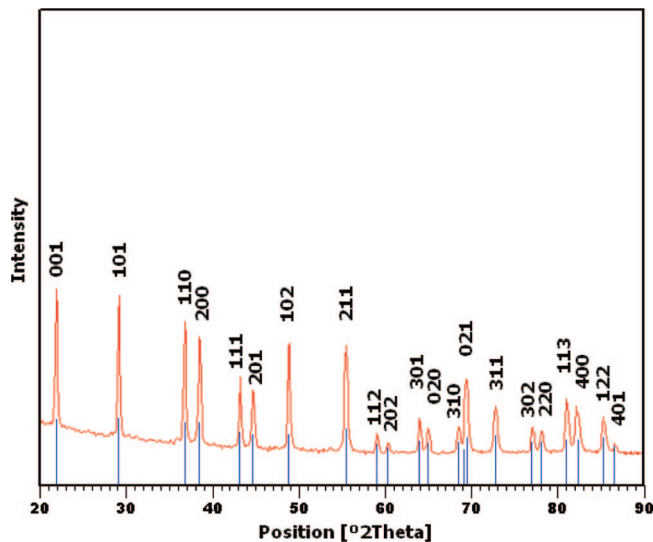


Figure 2. Powder X-ray diffraction pattern of an $Os_{0.8}Ru_{0.2}B_2$ solid solution indexed in accordance with the reference pattern of OsB_2 (JCPDS no. 00-017-0370).

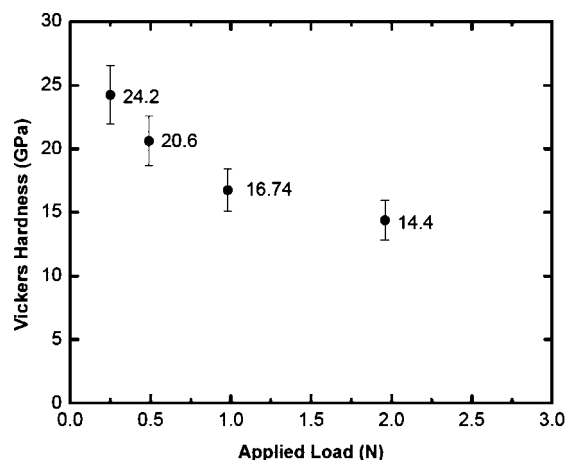


Figure 3. Vickers hardness of pure RuB_2 measured as a function of applied load.

compound is highly crystalline. The patterns were indexed according to the JCPDS reference pattern no. 00-015-0213. RuB_2 is orthorhombic (space group $Pmmn$) with the following lattice constants: $a = 4.6410\ \text{\AA}$, $b = 2.8630\ \text{\AA}$, $c = 4.0440\ \text{\AA}$. The powder patterns of the solid solutions, $Os_{1-x}Ru_xB_2$ were also highly crystalline and matched the JCPDS reference pattern for OsB_2 (Figure 2). Due to the fact that RuB_2 and OsB_2 have the same structure with almost equal lattice constants, both the reference patterns and experimentally observed powder diffraction patterns are nearly identical. Elemental analysis performed on the arc-melted pellets confirmed that the initial stoichiometry was reasonably well maintained for each sample. For example, EDS performed on three individual specimens indicated that the final composition of $Os_{0.8}Ru_{0.2}B_2$ was $81.8 \pm 1.4\%$ osmium and $18.2 \pm 1.4\%$ ruthenium.

Microindentation experiments were performed on RuB_2 and on the solid solutions of varying composition. The load-dependent hardness data for RuB_2 are presented in Figure 3. RuB_2 has a minimum hardness of 14.4 GPa at 1.96 N and a maximum measured hardness of 24.2 GPa at 0.25 N. For comparison, OsB_2 has an average hardness of 17.8 GPa

(25) Weinberger, M. B.; Cumberland, R. W.; Levine, J. B.; Conil, N.; Shahar, A.; Kaner, R. B.; Tolbert, S. H.; Kavner, A. *Phys. Rev. B* **2009**, submitted.

(26) Larson, A. C.; Von Dreele, R. B. *General Structure Analysis System (GSAS)*; Report LAUR 86-748; Los Alamos National Laboratory: Los Alamos, NM, 2000.

(27) Dorogokupets, P. I.; Dewaele, A. *High Pressure Res.* **2007**, 27 (4), 431-446.

at 1.96 N and 34.8 GPa at 0.25 N.¹⁸ The observed inverse relationship between the applied load and the measured hardness has been extensively documented and observed for many different types of materials. This phenomenon, referred to as the indentation size effect (ISE), is dominant only at low load. The ISE is primarily attributed to work hardening and strengthening effects arising from the presence of strain gradients under the indenter.^{28–30}

To avoid the effects of the ISE, it has been suggested that only load-independent hardness values be reported.³¹ However, although all materials exhibit the plateau from load-dependent to load-independent hardness values, it is interesting to note that its onset and magnitude from low to high loads vary among materials. In metals, metallic alloys, and ceramics, the hardness measured at low load is approximately 20% higher than measurements taken at loads where the hardness has plateaued.^{32–33} In contrast, OsB₂ and RuB₂ exhibit close to 50% reductions in hardness at high loads over low loads. This substantial difference suggests the potential for significant work hardening at lower loads in these transition metal borides. It is also interesting to compare the onset of the plateau for these transition metal diborides. For example, RuB₂ starts to plateau at approximately 2 N, whereas OsB₂ begins to plateau at approximately 5 N. This suggests that the end point of the ISE under a load-bearing tip is reached earlier for RuB₂ than for OsB₂, and therefore, it is possible that RuB₂ undergoes less work hardening than OsB₂.

The solid-solution hardness values are presented in panels a and b in Figure 4 for applied loads of 0.49 and 1.96 N, respectively. All of the hardness values for Os_{1-x}Ru_xB₂ fall between the values for the two end members, generally following Vegard's law within experimental error at both the lower and higher loads.³⁴ No solid-solution hardening is observed and there is no typical parabolic curve relating the dopant concentration to hardness. These results are contradictory to the typical hardness behavior of solid solutions and require some additional explanation.

Solid-solution hardening can be driven by different processes, including size-misfit of an additional element (as discussed previously) or changes in the valence electron count resulting from the additional element. Iridium superalloys for ultrahigh temperature applications presents a typical example of the first type of solid-solution hardening. Pure iridium metal has a Vickers hardness of 3.2 GPa. Incorporation of 3 mol % hafnium increases the hardness to 6.4 GPa and the addition of 5 mol % niobium increases the hardness to a maximum of 8.5 GPa for IrHf_{0.01}Nb_{0.05}.³⁵ Three factors were found to influence solid-solution hardening: the structural difference between Ir and the alloying element,

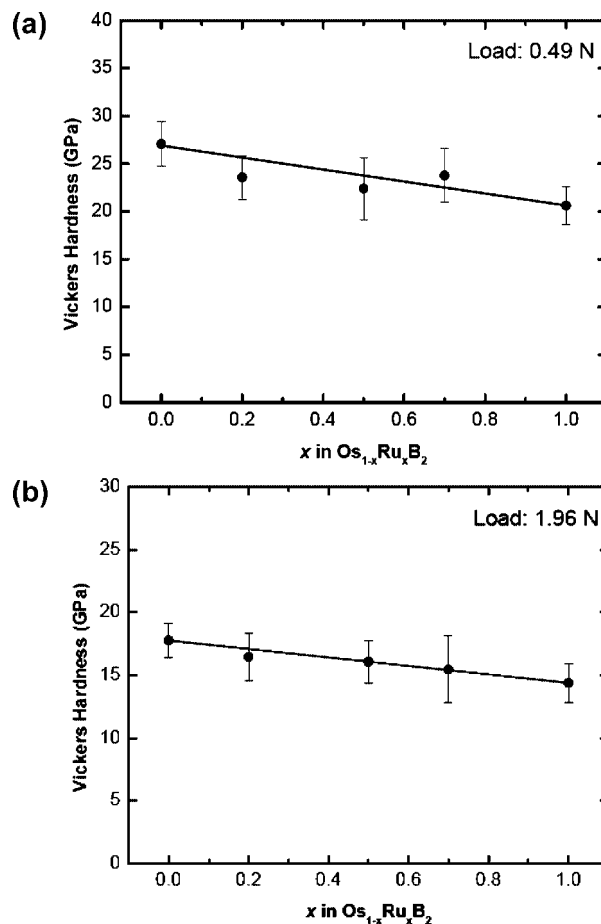


Figure 4. (a) Hardness of Os_{1-x}Ru_xB₂ as a function of osmium content measured under a load of 0.49 N. The solid line represents Vegard's Law. (b) Hardness of Os_{1-x}Ru_xB₂ as a function of osmium content measured under a load of 1.96 N. The solid line represents Vegard's Law.

the size misfit parameter, and the solubility limit of the alloying element. Hafnium and niobium have atomic radii 16.5 and 4.3% larger than iridium, respectively. This size misfit parameter is likely the most important parameter because the lattice distortion and solubility limit and thus the solid-solution hardening, are directly related to the differences in atomic radii.

Similar solid solution hardening has been observed in materials more closely related to our system, such as Nb_{1-x}Zr_xC. However, the hardening here is driven by changes in the number of valence electrons per formula unit, referred to as the valence electron concentration (VEC), resulting from the addition of Zr rather than a size misfit parameter. For this hard transition metal carbide, the maximum hardness is obtained at a dopant concentration of $x = 0.6$.²³ The substitution of Zr for Nb removes one electron from the unit cell, because Zr has one less valence electron than Nb. Thus, as one varies the zirconium concentration, the VEC is tuned accordingly. Theoretical studies revealed that the optimal dopant level of $x = 0.6$ results in completely filled σ bonding states between the p orbitals of carbon and metal d orbitals, which maximizes the bond covalency.²³ Thus, a VEC that deviates from 0.6, either by an excess or deficiency of zirconium, would result in under-populated bonding states or overpopulated antibonding states, respectively, both of which serve to destabilize the bond strength.

(28) Gao, H.; Huang, Y.; Nix, W. D. *Naturwissenschaften* **1999**, *86* (11), 507–515.

(29) Nix, W. D.; Gao, H. *J. Mech. Phys. Solids* **1998**, *46* (3), 411–425.

(30) Swadener, J. G.; George, E. P.; Pharr, G. M. *Mater. Res. Soc. Symp. Proc.* **2002**, *695*, 451–456.

(31) Brazhkin, V.; Dubrovinskaja, N.; Nicol, M.; Novikov, N.; Riedel, R.; Solozhenko, V.; Zhao, Y. *Nat. Mater.* **2004**, *3* (9), 576–577.

(32) Iost, A.; Bigot, R. *J. Mater. Sci.* **1996**, *31*, 3573.

(33) Farges, G.; Degout, D. *Thin Solid Films* **1989**, *181*, 365.

(34) Denton, A. R.; Ashcroft, N. W. *Phys. Rev. A* **1991**, *43* (6), 3161–4.

(35) Sha, J. B.; Yamabe-Mitarai, Y. *Scr. Mater.* **2006**, *54* (1), 115–119.

For the case of $Os_{1-x}Ru_xB_2$, ruthenium and osmium lie in the same column of the periodic table. As a result, the VEC remains constant regardless of the dopant concentration and no solid solution hardening is observed. Additionally, because both atoms have similar atomic radii and an equal number of valence electrons, the size misfit parameter and the change in the energy profile of nearest neighbors is expected to be small, maintaining the symmetric nature of kink motion. Thus, the hardness for this system simply follows Vegard's law with a minimum hardness for RuB_2 and a maximum hardness obtained for OsB_2 . Note that OsB_2 and RuB_2 are highly anisotropic materials. For example, both materials are highly anisotropic with respect to shear, as seen in calculations of the elastic shear anisotropy, A_G , determined by Hao, et al. from local density approximation (LDA) and generalized gradient approximation (GGA).³⁶ OsB_2 and RuB_2 both have the same orthorhombic crystal structure, however, and so we do not expect the hardness anisotropy or elastic anisotropy to be different in either end member or in the solid solutions.

Although the solid solutions appear to show fairly predictable behavior, significant insight can be gained by considering differences in the behavior of the end members. The microhardness of RuB_2 is 33% lower than that of OsB_2 , which is surprising considering the similarities between these two materials. Both compounds are orthorhombic and crystallize in the $Pmmn$ space group. They have identical valence electron counts, and nearly identical lattice constants and atomic positions. Electronic charge density and density of states calculations have shown that the covalent bonding in both compounds is due to strong overlap between the transition metal d orbitals and the 2p orbitals of boron.^{16,17,37,38} In fact, because of the slightly smaller covalent radius of ruthenium, 1.25 Å compared to 1.26 Å for osmium, one might even expect RuB_2 to be a harder material. Recent theoretical calculations using LDA calculations have actually predicted that RuB_2 possesses a shear constant, C_{44} (104 GPa), greater than the C_{44} for OsB_2 (79 GPa) and a shear modulus equal in magnitude to OsB_2 with a value of 187 GPa.³⁶ Because shear strength is highly correlated with hardness, we would expect RuB_2 and OsB_2 to have similar hardness values.^{1,4,5,39}

To explain this inconsistency, we propose that the increase in hardness for OsB_2 is due to relativistic effects that result in better orbital overlap and increased bond strength for the Os–B bonds compared to the Ru–B bonds. As the positive charge on a nucleus increases with higher atomic numbers, so too does the electrostatic attraction between the nucleus and the orbiting electrons. In order to compensate for the increase in attractive forces, the electrons must move faster to maintain their orbits and avoid getting pulled into the nucleus.⁴⁰ Einstein's theory of special relativity states that

matter and energy are intimately related and as objects begin to approach the speed of light their mass must increase accordingly. The increase in mass causes the 1s orbital to contract and the other s orbitals contract in turn because of the inverse relationship between the Bohr radius and mass.⁴¹ The d orbitals, which have very little electron density close to the nucleus and experience an increase in shielding by the relativistically contracted s orbitals, do not contract.⁴⁰ The velocity and mass increase for orbiting electrons only becomes significant for Z approximately equal to 50 and begins to affect bonding and reactivity for the transition metals at the end of the periodic table with Z approximately equal to 80.⁴²

The immediate effect of the relativistic contraction is that the orbital energies of Os and Ru differ. Because lower energy levels fill up first, these elements have different valence electron configurations: $Ru-[Kr]5s^14d^7$ and $Os-[Xe]6s^25d^6$. Calculations on the valence orbitals of the group 6 metals confirm that, for tungsten (Z = 74), the 6s orbital, which contracts, is lowered in energy and the 5d orbital, which expands, is raised in energy.⁴³ The change in energy levels for Mo (Z = 42) is insignificant. It is assumed that an analogous effect will occur for Ru (Z = 44) and Os (Z = 76). Relativistic calculations on the atomic orbitals of Os in the metal tetroxide confirm that the stabilization and contraction of the 6s orbital and a destabilization and expansion of the 5d orbital result in greater bond covalency for OsO_4 than for RuO_4 .⁴⁴ Similarly, relativistic effects were found to provide a greater increase in covalent bonding for OsF_6 when compared to RuF_6 .⁴⁵ The greater hardness of OsB_2 versus RuB_2 is believed to be a direct result of the relativistic expansion and contraction of the valence atomic orbitals of osmium. The expansion of the 5d orbital results in increased overlap with the 2p orbital of B, thus strengthening the Os–B bond. The Ru–B bonds in RuB_2 experience no such strengthening because ruthenium, with its low atomic mass, does not experience any significant relativistic effects. It should be emphasized that even though the 5d orbitals of osmium expand, this argument does not contradict our prior statement that ruthenium and osmium have similar atomic radii. This is because the outermost orbitals are the ns and np as opposed to the (n–1)d orbitals;⁴¹ in other words, for a given atomic radius, osmium has greater d electron density further away from the nucleus compared to ruthenium, improving the orbital overlap with the 2p orbitals of boron without increasing the overall radius of the osmium atom.

Relativistic effects may also contribute to the greater ISE of OsB_2 compared to RuB_2 . The ISE for OsB_2 results in a 96% increase in hardness from high load to low load, whereas RuB_2 increases by only 68%. Under low load, where plastic deformation has a greater dependency on intrinsic bond strength (rather than extrinsic factors), the Os–B bonds

(36) Hao, X.; Xu, Y.; Wu, Z.; Zhou, D.; Liu, X.; Meng, J. *J. Alloys Compd.* **2008**, *453* (1–2), 413–417.

(37) Hao, X. F.; Wu, Z. J.; Xu, Y. H.; Zhou, D. F.; Liu, X. J.; Meng, J. *J. Phys.: Condens. Matter* **2007**, *19*, 196212.

(38) Hebbache, M.; Stuparevic, L.; Zivkovic, D. *Solid State Commun.* **2006**, *139* (5), 227–231.

(39) Brazhkin, V. V.; Lyapin, A. G.; Hemley, R. J. *Philos. Mag., A* **2001**, *82*, 231.

(40) Bond, G. C. *Platinum Met. Rev.* **2000**, *44* (4), 146–155.

(41) Huheey, J. E.; Keiter, E. A.; Keiter, R. L., *Inorganic Chemistry: Principles of Structure and Reactivity*, 4th ed.; HarperCollins College Publishers: New York, 1993.

(42) Onoe, J.; Sekine, R.; Takeuchi, K.; Nakamatsu, H.; Mukoyama, T.; Adachi, H. *Chem. Phys. Lett.* **1994**, *217* (1–2), 61–4.

(43) Hoffman, D. C.; Lee, D. M. *J. Chem. Educ.* **1999**, *76* (3), 332–347.

(44) Pershina, V.; Bastug, T.; Fricke, B. *J. Chem. Phys.* **2005**, *122* (12), 124301/1–124301/9.

(45) Onoe, J. *J. Phys. Soc. Jpn.* **1997**, *66* (8), 2328–2336.

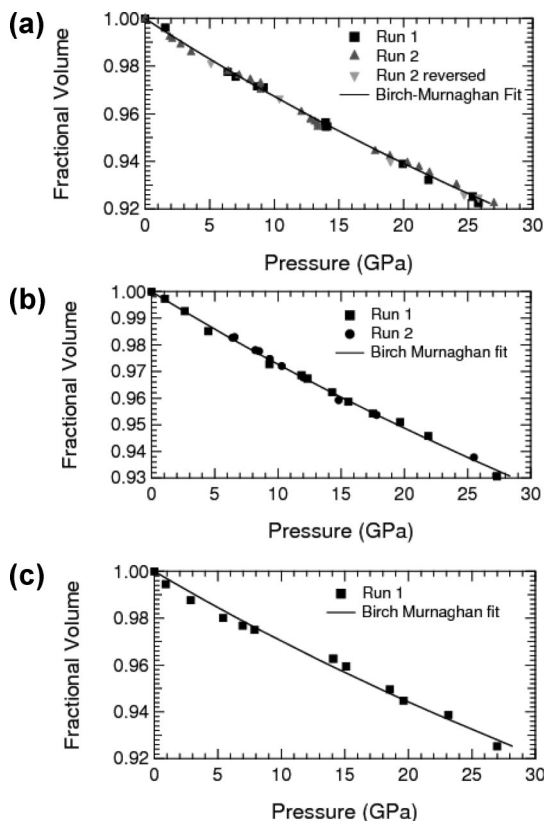


Figure 5. (a) Pressure vs fractional volume change for RuB₂. Fitting this data with a third-order Birch–Murnaghan equation of state results in a bulk modulus of 281 GPa. (b) Pressure vs fractional volume change for Os_{0.8}Ru_{0.2}B₂. Fitting this data with a 3rd order Birch–Murnaghan equation of state results in a bulk modulus of 342 GPa. (c) Pressure vs fractional volume change for Os_{0.5}Ru_{0.5}B₂. When fit with a third-order Birch–Murnaghan equation of state this data yields a bulk modulus of 311 GPa. Error in the fractional volume determination is within the size of each data-point.

provide greater resistance to deformation, resulting in a higher hardness and thus a greater ISE compared to RuB₂.

In addition to trends in hardness, we can also examine trends in bulk modulus across the solid solution samples. Analysis of the high pressure X-ray diffraction data results in the determination of the bulk modulus for each material. The pressure vs fractional volume data of RuB₂ as well as the two studied solid solutions were fit using the third-order Birch–Murnaghan equation of state to determine both the zero pressure bulk modulus (B_0) and its derivative with respect to pressure (B_0'). When B_0' is fixed to the canonical value of 4, the bulk moduli of RuB₂, Os_{0.5}Ru_{0.5}B₂, and Os_{0.8}Ru_{0.2}B₂ are 281, 311, and 342 GPa, respectively (Figure 5a–c). As we previously reported, the bulk modulus of OsB₂ is 365 GPa (when B_0' is set to 4).⁸ A bulk modulus of 242 GPa was recently reported for RuB₂ with a B_0' value of 5.2.⁴⁶ The bulk moduli of the solid solutions are very close to that expected for linear combinations of the end member bulk moduli, again, in accordance with Vegard's law (Figure 6). The applicability of Vegard's law to this system is logical, given the close proximity of the constituent elements in the periodic table, their similar size, and comparable chemical behavior. From the data, we can conclude that the bulk

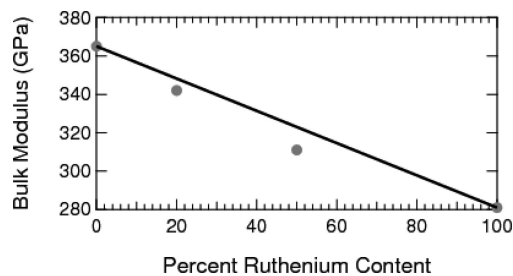


Figure 6. Percent ruthenium content vs bulk modulus. As the percentage of ruthenium in the diboride is increased, the bulk modulus of the solid solution decreases in accordance with Vegard's Law.

moduli of these transition metal diborides scale linearly with composition.

Although the linear scaling of the solid solutions is quite reasonable, we again need to consider the origin of the differences in the bulk modulus values obtained for the two pure end members. In doing so, the common structural features of OsB₂ and RuB₂ enable us to isolate the effects of VED on bulk modulus. The VED of OsB₂ is $0.512 \text{ e}^-/\text{\AA}^3$ and that of RuB₂ is $0.521 \text{ e}^-/\text{\AA}^3$, leading us to predict that these two compounds should have similar bulk moduli. Yet, despite their nearly identical valence electron densities, the bulk moduli values differ by 23%, which seemingly contradicts the belief that bulk modulus is proportional to VED.

To a first approximation, VED remains proportional to incompressibility (see, for example, Figure 12.4 in ref 2); however, at high pressures, we believe that core electron density plays a secondary role in determining bulk modulus. Referring back to the parent metals, ruthenium and osmium both have comparable VEDs of 0.59 and $0.572 \text{ e}^-/\text{\AA}^3$, respectively, yet vastly different bulk moduli, 348 GPa⁹ and 395–462 GPa. A similar scenario can be found in the pair of group 4 transition metal carbides, NbC and TaC. These isostructural and isovalent carbides (cubic, space group $Fm\bar{3}m$) have nearly identical lattice constants, and VEDs of 0.403 and $0.407 \text{ e}^-/\text{\AA}^3$, respectively. However, the bulk modulus of NbC is only 274 GPa and that of TaC_{0.98} is 345 GPa.^{47,48} In this case, the additional core electrons of Ta result in a 24% increase in bulk modulus for TaC_{0.98} compared to NbC.

We postulate that under extreme pressures, the additional 32 core electrons of osmium increase the repulsive electrostatic forces between atoms and result in the greater incompressibility of OsB₂ compared to RuB₂. Note that the higher cohesive energy and relativistic contraction of the s orbitals in osmium may also contribute to the resistance in isotropic compression for OsB₂.⁴⁹ To a first approximation, VED provides an accurate measure for comparing bulk moduli; however, for atoms with substantially different electronic cores, total electron density (TED) should be considered as a perturbation on VED. Thus, it follows that the bulk moduli of the solid solutions should follow Vegard's law because the TED should scale with osmium concentration.

(46) Gu, Q.; Krauss, G.; Steurer, W. *Adv. Mater.* **2008**, *20*, 3620.

(47) Liermann, H. P.; Singh, A. K.; Manoun, B.; Saxena, S. K.; Zha, C. S. *Int. J. Refract. Met. Hard Mater.* **2005**, *23* (2), 109–114.

(48) Liermann, H. P.; Singh, A. K.; Somayazulu, M.; Saxena, S. K. *Int. J. Refract. Met. Hard Mater.* **2007**, *25* (5–6), 386–391.

(49) Gschneidner, K. A. Physical Properties and Interrelationships of Metallic and Semimetallic Elements. In *Solid State Physics*; Seitz, F., Turnbull, D., Eds.; Academic Press: New York, 1964; Vol. 16, pp 276–388.

Conclusions

We have synthesized RuB_2 and the solid solutions $Os_{1-x}Ru_xB_2$ in order to test the effect of a secondary metal in these ultra-incompressible hard borides. The compounds were studied by in situ high pressure X-ray diffraction and Vickers hardness. RuB_2 was found to have a bulk modulus of 281 GPa and a load-dependent hardness that ranges from 14.4 to 24.2 GPa. The solid solutions obey Vegard's law with hardness values and incompressibilities that vary linearly with composition.

Examination of the trends in hardness and bulk modulus across compositions provides insight into the electronic structural components that control each property. The dominant mechanism for increasing hardness in this system appears to be the bond strength of Os–B, which is postulated to be stronger than Ru–B, because of the relativistic effects of Os increasing bond overlap for the 5d and 2p orbitals of Os and B, respectively. The strength of the covalent bonds presents a stronger energetic barrier to deformation than the variation in the electronic field resulting from elemental substitutions, preventing significant solid-solution hardening.

The trends in bulk modulus can be explained by the

postulate that total electron density, in addition to valence electron density, is important in controlling repulsive interactions between atoms. OsB_2 has both a higher total electron density and a higher bulk modulus than RuB_2 . The observed linear scaling of the bulk moduli of the solid solutions is reasonable, following Vegard's law. Thus, although these results do not show that the formation of solid solutions is a good method to improve the hardness of OsB_2 , they do significantly refine our design parameters. This should be useful in the future design of new hard materials, particularly in assessing the pros and cons of employing heavier transition metals.

Acknowledgment. The authors thank Martin Kunz and Sander Caldwell for their assistance in completing this work. This work was funded by the National Science Foundation under grants CMS-0307322 (SHT), DMR-0453121 (RBK) and DMR-0805357 (RBK/SHT). The Advanced Light Source is supported by the Director, Office of Science, Office of Basic Energy Sciences, Materials Sciences Division, of the U.S. Department of Energy under Contract DE-AC03-76SF00098 at Lawrence Berkeley National Laboratory.

CM900211V